J Biomol NMR (2013) 57:305–311
DOI 10.1007/s10858-013-9790-2

ARTICLE

Equivalence between Euler angle conventions for the description of tensorial interactions in liquid NMR: application to different software programs

Patrice Dosset · Philippe Barthe · Martin Cohen-Gonsaud · Christian Roumestand · Hélène Déméné

Received: 21 June 2013 / Accepted: 9 October 2013 / Published online: 17 October 2013

Abstract Long-range orientational restraints derived from alignment or rotational diffusion tensors have greatly contributed to the expansion of applications in biomolecular NMR. The orientation of the principal axis system of these tensors is usually described by the so-called Euler angles. However, no clear consensus has emerged concerning the convention of the associated orthogonal rotations. As a result, the different programs that derive or predict them have adopted different conventions, which make comparison between their results difficult. Moreover, the rotation schemes are seldom completely described. Here, we summarize the different conventions, determine which ones are adopted by commonly used software packages, and establish the formal equivalencies between the different calculated Euler angles.

Keywords Euler angles · Rotation axes · Convention · Mobile axes · Fixed axes · Passive and active rotations

Abbreviations

PAS	Principal axis system
RCSA	Residual chemical shift anisotropy
RDC	Residual dipolar couplings

Electronic supplementary material The online version of this article (doi:10.1007/s10858-013-9790-2) contains supplementary material, which is available to authorized users.

P. Dosset · P. Barthe · M. Cohen-Gonsaud · C. Roumestand · H. Déméné (✉)
CNRS UMR 5048, Centre de Biochimie Structurale, Université de Montpellier 1 et 2, 29, rue de Navacelles, 34090 Montpellier, France
e-mail: helene.demene@cbs.cnrs.fr

P. Dosset · P. Barthe · M. Cohen-Gonsaud · C. Roumestand · H. Déméné
INSERM U1054, 34090 Montpellier, France

Introduction

During the past decades, one of the principal advances in theoretical and computational biomolecular NMR spectroscopy concerned the introduction of long-range orientational restraints. One can cite residual dipolar couplings (RDCs) (Tjandra and Bax 1997; Tjandra et al. 1997b), heteronuclear relaxation rates (Tjandra et al. 1997a), and residual chemical shift anisotropies (RCSAs) (Cornilescu and Bax 2000). Among others things, these restraints are particularly useful for the structural analysis of multi-domain proteins, as long-range distances enable the determination of the relative orientation of two domains when the number of short inter-proton distances (<5 Å) between the domains is limited. The study of protein complexes could also benefit from long-range distance information, when it is difficult to observe intermolecular NOEs. This phenomenon is due to the intrinsic sensitivity of experiments used to measure heteronuclear separated/filtered NOEs, which fall off rapidly when the molecular weight increases. Alternatively, lack of NOE signals could be due to unfavorable side chain dynamics at the interface, resulting in the broadening of interfacial side chain resonances and subsequent NOEs quenching.

RDCs can be measured if the molecule is partly aligned with the magnetic field, so that its alignment tensor **A** is not null and is anisotropic. In the case of diamagnetic molecules, this is generally achieved by the introduction of anisotropic alignment media, such as filamentous bacteriophage Pf1 (Hansen et al. 1998), phospholipid bicelles (Tjandra and Bax 1997) or ether/alcohol bilayers (Ruckert

and Otting 2000). Likewise, the relaxation rates can be translated into long-range restraints if the molecule tumbles anisotropically in solution, reflecting that the eigenvalues of its rotational diffusion tensor **D** are not equal. Both tensors are fully characterized by the orientation of their principal axes, as reported by the Euler angles, and by their eigenvalues. It is well known that if the nature of the alignment process is steric, the orientation of both tensors is similar and their comparison can thus serve as cross-validation. For example, the similarity of Euler angles between the **A** and **D** tensors demonstrated that the RNA-binding module of the modular LicT protein was monomeric in its inactive form (Déméné et al. 2008), contrary to what observed for structures of RNA-binding domains from proteins of this family (Manival et al. 1997; van Tilbeurgh et al. 1997; Yang et al. 2002). Likewise, the comparison between the steric alignment tensor and the rotational diffusion tensor confirmed that the β-cyclodextrin-loaded maltose binding protein experienced a conformational rearrangement of its two domains in solution when compared to the X-Ray structure (Hwang et al. 2001; Skrynnikov et al. 2000). The comparison between the predicted alignment tensor (Almond and Axelsen 2002; Azurmendi and Bush 2002; Fernandes et al. 2001; Ferrarini 2003; Wu et al. 2006; Zweckstetter and Bax 2000; Zweckstetter et al. 2004) and the alignment tensor estimated from experimental dipolar couplings is also of interest whether the interactions between the macromolecular solute and the nematogenic particles are purely steric or contain an electrostatic contribution. Hence, the measurement of D_{HN} RDCs in phospholipid bicelles and their simulation with the PALES software (Zweckstetter and Bax 2000) established that the orientation of the two sub-units of the dimeric cyanovirin-N was different in the crystal and in the solution structures (Bewley and Clore 2000). Likewise, comparison between RDCs measured in Pf1 phage solution and RDCs calculated with the PALES software package enabled the determination of the packing mode (parallel vs. antiparallel) of the coiled-coil domain of cGMP protein kinase (Zweckstetter et al. 2005). Recent studies have also established the possibility to validate the protein orientation within a complex by comparison of predicted and experimentally-determined alignment (Berlin et al. 2010) or diffusion (Ryabov and Fushman 2007; Ryabov et al. 2009) tensors. Finally, there is a general tendency to validate the solution structure of high molecular weight proteins with predicted versus experimental NMR-derived tensors (Vincent et al. 2012).

A characteristic of these long-range restraints is that they provide direct geometric information on the orientation of interatomic vector(s) with respect to the principal axis system (PAS) of the related tensor. PAS orientations are reported by the so-called Euler angles. The software packages commonly used to calculate or predict Euler angles have been developed by different research teams who have adopted different conventions, often with little, if any, documentation, thus precluding direct comparison between them. In addition, no laboratory has developed a complete set of programs which both predict (from a structure) and derive (from experimental data) the diffusion and alignment tensors, making difficult any cross-validation. Blackledge's team has developed two widely used software packages, MODULE and TENSOR2 to derive the alignment and the diffusion tensors, respectively, from NMR experimental data, but no program to predict them from the structure of the molecule. Hence, other software packages, developed in other groups with other rotation conventions, must be used to achieve that prediction, with the risk of misinterpreting data.

In the present manuscript, we have established the rotation conventions adopted in commonly used programs: r2r1 (http://www.palmer.hs.columbia.edu/software/r2r1_diffusion.html), ROTDIF (Blake-Hall et al. 2004; Fushman et al. 1999; Ghose et al. 2001; Walker et al. 2004), (http://gandalf.umd.edu/FushmanLab/pdsw.html), TENSOR2 (Dosset et al. 2000) (http://www.ibs.fr/science-213/scientific-output/software/tensor/), REDCAT (Valafar and Prestegard 2004) (http://ifestos.cse.sc.edu/software), MODULE (Dosset et al. 2001) (http://www.ibs.fr/science-213/scientific-output/software/module/), Xplor-NIH (Schwieters et al. 2003) (http://nmr.cit.nih.gov/xplor-nih/), PALES (Zweckstetter and Bax 2000; Zweckstetter et al. 2004) (http://www3.mpibpc.mpg.de/groups/zweckstetter/_links/software_pales.htm) and DCserver (http://spin.niddk.nih.gov/bax/nmrserver/dc), as well as their formal equivalencies. These conventions were verified on experimental data collected on the extracellular PASTA domains of the PknB protein which NMR structure was previously solved in the laboratory (Barthe et al. 2010).

Theory

The diffusion and alignment tensors are defined by their PAS, where the matrix adopts a diagonal form. There are infinite ways to combine rotations to move a reference frame, here the molecule-fixed frame, to the PAS. Usually, the orientation of the PAS is described by the 3 Euler angles (α, β, γ) which define the three rotations successively performed about three orthogonal axes so that the molecule-fixed frame (x, y, z) is transformed into three successive (X, Y, Z), (X′, Y′, Z′) and (X″, Y″, Z″) frames. The fourfold degeneracy of the Euler angles defining the orientation of the diffusion and alignment tensors that fulfills the experimental data has been largely documented. It corresponds to the different ways to orient the PAS axes,

while keeping the frame direct (X″, Y″, Z″), (−X″, −Y″, Z″), (X″, −Y″, −Z″), and (−X″, Y″, −Z″) and the second rank spherical harmonics, which describe the orientations of the vectors in the PAS, invariant. Less documented is the fact that to this fourfold degeneracy correspond numerically 8 Euler angles triplets: (α, β, γ) (1), (α, β, γ + π) (2), (α + π, π − β, −γ) (3), (α + π, π − β, π − γ) (4), (α + π, −β, γ) (5), (α + π, −β, γ + π) (6), (α, π + β, −γ) (7), (α, π + β, π − γ) (8), and not four as usually listed. In this list, which we will call **set A** thereafter, the four last numerical solutions correspond physically to the first four (not necessarily in that order, depending on the rotation scheme described below), contrary to the eight solutions listed for planar motifs (Hus et al. 2008; Mueller et al. 2000), which represent eight different physical solutions.

Another ambiguity comes from the fact that the convention defining the rotation axes themselves varies among authors and is not always detailed. Some have adopted the convention used in classical mechanics, where the rotations are performed successively around the (Z, X′, Z″) axes, whereas others have adopted the convention of quantum mechanics where the rotations are performed around the (Z, Y′, Z″) axes.

Another ambiguity derives from the difference between passive and active rotations, which can be roughly thought of as the difference between bringing the reference system into coincidence with the PAS or bringing the PAS into coincidence with the reference system by applying the Euler rotations (Schmidt-Rohr and Spiess 1994). In a passive rotation, the reference frame of the biomolecule is rotated until it coincides with the PAS, while in an active rotation, the PAS is rotated until it matches the biomolecule reference frame. From a mathematical point of view, the corresponding matrices are the inverse of each other. A detailed description of passive/active rotations, and of the confusion about Wigner matrices associated with them in the literature, has been recently published (Mueller 2011).

Another discrepancy between the different programs derives from the choice of either mobile or fixed rotation axes. The mathematical or graphical description of the transformation establishes that performing the rotations around the successively rotated axes α(Z), β(Y′) or β(X′), and γ(Z″), a transformation that we will call rotation about mobile axes thereafter, is equivalent to performing the successive rotations γ(z), β(y) or β(x), α(z) around the fixed axes of the original reference frame, here the (x, y, z) molecular frame (Rose 1955). As a consequence, the nomenclature used to define the angles should be reversed between the mobile and fixed axes conventions. If not, assuming passive rotations, the position of the tensor axis associated with the axial component is defined by the (α, β) doublet in the mobile convention and by the (γ, β) doublet in the fixed convention. Similarly, the planar position of the rhombic component is defined by the γ and α angles in the mobile and fixed conventions, respectively. For active rotations, it is the inverse: the axial component position is defined by the (γ, β) and (α, β) doublet in the mobile and fixed conventions, respectively, whereas the γ and α angles define the planar position of the rhombic components. The **set A** of equations mentioned above applies to the passive rotations about mobile axes as well as to the active rotations about fixed axes. For passive rotations about fixed axes and active rotations about mobile axes, the set of the eight degenerate solutions is (**set B**): (α, β, γ), (α + π, β, γ), (−α, π − β, γ + π), (−α + π, π − β, γ + π), (α, −β, γ + π), (α + π, −β, γ + π), (−α, π + β, γ), (−α + π, π + β, γ).

Finally, the tensor orientation is sometimes described by successive rotations about three different orthogonal axes, once about the x axis, once about the y axis, and once about the z axis. These angles, improperly referred as Euler angles, are known as the Tait–Bryan angles. Assuming passive rotations about mobile axes, the eight degenerate solutions can be constructed using **Set C** of equations: (α, β, γ), (α, β, γ + π), (α, π + β, −γ), (α, π + β, −γ + π), (α + π, π − β, γ), (α + π, π − β, γ + π), (α + π, −β, −γ), (α + π, −β, −γ + π).

All the foregoing assumes positive rotations, where a π/2 rotation about the z axis rotates the x axis counterclockwise to the y axis. A negative rotation will rotate it onto the—y axis.

Materials and methods

The extracellular construct comprising the four PASTA domains (residue 355–626) was purified as described in the original paper (Barthe et al. 2010). All NMR experiments were recorded at 310 K on a 700 MHz Bruker AVANCE

Table 1 Euler angles calculated[a] with different software packages for alignment tensor (measured in Pin 3 % $C_{12}E_5$/hexanol) and diffusion tensors of the PASTA12 bi-domain from PknB extracellular domain

Software	Euler angles[a]	Tensor nature[b]
MODULE	−58.1, 83.9, 77.0	**A**
Xplor-NIH	77.0, 83.9, 121.9	**A**
REDCAT	167.0, 96.1, −31.8	**A**
PALES (fit)	148.1, 84.0, 193.0	**A**
DCserver	−64.7, −75.7, 33.4	**A**
PALES (prediction)	125.7, 88.3, 187.4	**A**
TENSOR2	−23.6, 70.4, 77.3	**D**
ROTDIF	167.0, 109.2, 113.1	**D**

[a] As given by the software programm. The optimization of the tensors was performed against the first NMR model taken from the 2KUD PDB file. The prediction of the tensor with PALES was based on the 25th NMR model taken from the 2KUI PBD file, and oriented as the KUD structure

[b] **A** stands for alignment tensor, **D** for diffusion tensor

Table 2 Definition of Euler rotations for different software packages

Software programm	Tensor	Documented type	Effective rotation found	Documented axes found	Effective axis	Passive/active
Module	A	None	z, x, z	None	Fixed	Passive
Xplor-NIH	A	None	Z, X′, Z”	None	Mobile	Passive
RedCat	A	None	Z, Y′, Z”	None	Mobile	Passive
Pales	A	Z, Y′, Z”	Z, Y′, Z”	Mobile	Mobile	Active
DCserver	A	x, y, z	x, y, z	Fixed	Fixed	Active
r2r1[a]	D	None	Z, Y′	None	Mobile	Passive
Tensor	D	None	z, x, z	None	Fixed	Passive
Rotdif	D	Z, Y′, Z”	Z, Y′, Z”	Mobile	Mobile	Passive

[a] r2r1 determines the rotational diffusion tensor with an axially symmetric model

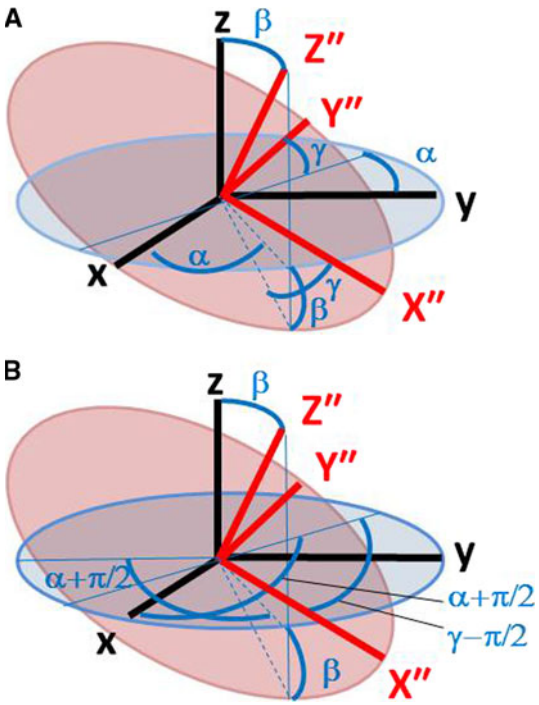

Fig. 1 Equivalence of Euler angles between the (*Z*, *Y*′, *Z*”) and the (*Z*, *X*′, *Z*”) rotation schemes (passive positive rotation, mobile axes). For clarity, only the initial (*X*, *Y*, *Z*) and the final (*X*”, *Y*”, *Z*”) frames are represented

III spectrometer equipped with a cryoprobe optimized for proton detection. D_{HN} dipolar couplings were measured as differences between J_{HN} splittings along the ω1 dimension in IPAP-HSQC experiments recorded in the original buffer (25 mM sodium acetate, pH 4.6) and in this buffer supplemented with 3 % $C_{12}E_5$/hexanol (Ruckert and Otting 2000). R1, R2, and NOE relaxation experiments were measured in the same experimental conditions. To ascertain the convention used in the different software packages, alignment and rotational tensors were derived from experimental data with in-house programs using the various rotation schemes described in the theory section (Déméné et al. 2000, 2002, 2008).

Results and discussion

R1, R2, NOE relaxation parameters and D_{HN} dipolar couplings were measured on the extracellular part of the PknB protein, which consists of four structurally homologous PASTA domains (PASTA1–PASTA4) (Barthe et al. 2010) ranging from residue 351 to 626. The experimental profiles are presented in supplementary material (Figs. S1, S2). Even if experimental data were recorded on the full 4-domain protein, the diffusion and alignment tensors were optimized on the better defined NMR structure of the bi-domain construct (PASTA12, residue 354–492). RDC predictions were obtained using the NMR structure of the full-length construct (PASTA1234), giving to the two first domains the same orientation as in the PASTA12 structure. Table 1 lists the Euler angles for the alignment and diffusion tensors calculated from experimental data: all the software packages tested yield different values for both tensors. For example, the β angle for the alignment tensor calculated by MODULE, Xplor-NIH, and PALES is the same (83.9, 83.9, 84.0), but the values of the α and γ angles are different, and cannot be deduced from each other from the eight relationships listed in the Theory section. The β value reported by REDCAT (96°) could be the complement to 180° of the 84° value given by Xplor-NIH, and PALES, but the α and γ values appear to have no correlation with the values calculated with the other programs. No obvious relation can be found between alignment tensors calculated with DCserver and the other software packages. DCserver is peculiar, as it reports the tensor orientation with Tait–Bryan angles (although called Euler angles) deduced from successive rotations about the x, y, z axes. Likewise, the Euler angles estimated for rotational diffusion tensors by ROTDIF and TENSOR2 cannot be deduced from each other with the eight expressions listed in the theory section to describe the Euler angle degeneracy.

The quasi identity between the D_{HN} values back-calculated by the different software packages stems from the fact that the derived tensors must be identical (Fig. S3, Supplementary Material).

Table 3 Correspondence between Euler angles (α_p, β_p, γ_p) as calculated by each software program and Euler angles (α_{ref}, β_{ref}, γ_{ref}) calculated with the convention of passive positive rotations about mobile axes with successive rotations around z, Y, Z′[a]

Software package	(α_p, β_p, γ_p)[b] Euler angles as calculated by the software program as a function of (α_{ref}, β_{ref}, γ_{ref})	(α_{ref}, β_{ref}, γ_{ref}) as a function of (α_p, β_p, γ_p)	Set of equations to construct the 8 degenerate solutions from the (α_p, β_p, γ_p) values
MODULE	$\gamma_{ref} - \pi/2$, β_{ref}, $\alpha_{ref} + \pi/2$	$\gamma_p - \pi/2$, β_p, $\alpha_p + \pi/2$	B
Xplor-NIH	$\alpha_{ref} + \pi/2$, β_{ref}, $\gamma_{ref} - \pi/2$	$\alpha_p - \pi/2$, β_p, $\gamma_p + \pi/2$	A
REDCAT	α_{ref}, β_{ref}, γ_{ref}	α_p, β_p, γ_p	A
PALES	$-\gamma_{ref}$, $-\beta_{ref}$, $-\alpha_{ref}$	$-\gamma_p$, $-\beta_p$, $-\alpha_p$	B
DCserver	$-\text{atan2}[(\sin\alpha_{ref}\sin\beta_{ref})/\cos\beta_{ref}]$[c], $-\arcsin[\cos\alpha_{ref}\sin\beta_{ref}]$, $\frac{-arctan\left[cos\alpha_{ref}cos\beta_{ref}sin\gamma_{ref}+sin\alpha_{ref}cos\gamma_{ref}\right]}{\left[cos\alpha_{ref}cos\beta_{ref}cos\gamma_{ref}-sin\alpha_{ref}sin\gamma_{ref}\right]}$	$\text{atan2}[(-\sin\alpha_p\cos\beta_p)/\sin\beta_p]$[c], $\arccos[\cos\alpha_p\cos\beta_p]$, $\frac{-arctan\left[(cos\alpha_p\sin\beta_p sin\gamma_p-sin\alpha_p cos\gamma_p\right]}{sin\alpha_p sin\gamma_p+cos\alpha_p sin\beta_p cos\gamma_p}$	C
TENSOR2	$\gamma_{ref} - \pi/2$, β_{ref}, $\alpha_{ref} + \pi/2$	$\gamma_p - \pi/2$, β_p, $\alpha_p + \pi/2$	B
ROTDIF	α_{ref}, β_{ref}, γ_{ref}	α_p, β_p, γ_p	A
r2r1	α_{ref}, β_{ref}	α_p, β_p	A

[a] In this convention, the unit vectors defining the tensor axes have the following coordinates: ($\cos\alpha_{ref}\cos\beta_{ref}\cos\gamma_{ref} - \sin\alpha_{ref}\sin\gamma_{ref}$, $-\cos\alpha_{ref}\cos\beta_{ref}\sin\gamma_{ref} - \sin\alpha_{ref}\cos\gamma_{ref}$, $\cos\alpha_{ref}\sin\beta_{ref}$), ($\sin\alpha_{ref}\cos\beta_{ref}\cos\gamma_{ref} + \cos\alpha_{ref}\sin\gamma_{ref}$, $-\sin\alpha_{ref}\cos\beta_{ref}\sin\gamma_{ref} + \cos\alpha_{ref}\cos\gamma_{ref}$, $\sin\alpha_{ref}\sin\beta_{ref}$), ($-\cos\beta_{ref}\cos\gamma_{ref}$, $\sin\beta_{ref}\sin\gamma_{ref}$, $\cos\beta_{ref}$)

[b] The eightfold numerical degeneracy of Euler angles mentioned in the text still holds, irrespective of the second rotation axis. However, since the eightfold degeneracy of Euler angles was detailed assuming that the rotation axes are mobile, care must be taken to reverse the angles α and γ if the software uses the convention of fixed axes. If one takes the case of the Euler angles reported by Module, the eight corresponding Euler triplets for the passive rotation about mobile axes are (Y rotation): ($\gamma_p - \pi/2$, β_p, $\alpha_p + \pi/2$) (1), ($\gamma_p - \pi/2$, β_p, $\alpha_p + 3\pi/2$) (2), ($\gamma_p + \pi/2$, $\pi - \beta_p$, $-\alpha_p - \pi/2$) (3), ($\gamma_p + \pi/2$, $\pi - \beta_p$, $\pi/2 - \alpha_p$) (4), ($\gamma_p + \pi/2$, $-\beta_p$, $\alpha_p + \pi/2$) (5), ($\gamma_p + \pi/2$, $-\beta_p$, $\alpha_p + 3\pi/2$) (6), ($\gamma_p - \pi/2$, $\pi + \beta_p$, $-\alpha_p - \pi/2$) (7), (α_p, $\pi + \beta_p$, $\pi/2 - \alpha_p$) (8)

[c] The atan2 function of a quotient (a/b) takes into account the signs of a and b and returns the computed angle in the appropriate quadrant (modulo 2π)

Table 4 Euler angles calculated[a] with different software packages for the alignment tensor (measured in Pin 3 % $C_{12}E_5$/hexanol) and the rotational diffusion tensor of the PASTA12 bi-domain from PknB extracellular domain

Software package	Calculated Euler angles[a]	Harmonized Euler angles[b]
MODULE	−58.1, 83.9, 77.0	167.0, 96.1, −31.9 (3)
Xplor-NIH	77.0, 83.9, 121.9	167.0, 96.1, −31.9 (4)
REDCAT	167.0, 96.1, −31.8	167.0, 96.1, −31.8 (1)
PALES (fit)	148.1, 84.0, 193.0	167.0, 96.0, −31.9 (8)
DCserver	−64.7, −75.7, 33.2	167.0, 96.1, −32.0 (3)
PALES (prediction)	125.7, 88.3, 187.4	172.6, 91.7, −54.3 (8)
TENSOR2	−23.6, 70.4, 77.3	167.3, 109.6, −66.4 (3)
ROTDIF	167.0, 109.2, 113.1	167.0, 109.2, −66.9 (2)

[a] As given by the software package. The optimization of the tensors was performed against the first NMR model taken from the 2KUD PDB file. The prediction of the tensor with PALES was based on the first NMR model taken from the 2KUI PBD file

[b] The number into brackets refers to one of the 8 Euler angles triplets listed in the text (**set A**) that was used to establish the equivalence after application of transformations according to Table 3

We attempted next to find the Euler convention used by these different programs. The results are listed in Table 2, as well as the documentation found. Only ROTDIF gives explicitly the rotation matrix to transform the coordinates from the molecule-fixed frame to the diffusion frame (Ghose et al. 2001), and can be thus considered as giving the full description of its Euler angle convention: Y′ convention, mobile axis, and passive rotation. PALES provides details only for the second rotation axis (Y′), and no documentation is available for the other programs, with the exception of DCserver. As listed in Table 2, we find that most software packages have adopted different conventions, thus explaining the discrepancies seen in Table 1. A special case is DCserver, which uses successive rotations about three orthogonal different axes x, y, z. As documented, we found rotations about mobile axes, but with the active convention. Alternately, DCserver could be considered as performing passive negative rotations about fixed axes. TENSOR2, MODULE, Xplor-NiH (subroutine CalcTensor), do define their transformations as Z, X′, Z″ successive rotations, but TENSOR2 and MODULE reason in terms of fixed axes while Xplor-NIH does so in terms of the mobile convention. PALES and REDCAT use the Y rotation axis, but with the active and passive conventions, respectively. Finally, we found that all software packages investigated in this study, except PALES and DCserver, have adopted the active rotation convention.

To be able to compare the Euler angles between the different rotation schemes, the equivalence between X′ and Y′ rotation was investigated. Fig. 1 depicts Euler angles

Y′- and X′-based Euler transformations yielding the same final orientation. From this graph, one can see that performing a α(Z), β(Y′), γ(Z″) rotation is equivalent to performing a α + π/2(Z), β(Y′), γ − π/2(Z″) rotation. There is not such a simple equivalence between Euler angles and Tait–Bryan angles, and the conversion formula was derived from the transformation matrices. Taking these results into account, Table 3 lists the equivalences between the different conventions used by the different programs. From a formal point of view, according to the terminology adopted by Wolf (1969), performing a positive passive rotation about mobile axes is equivalent to performing an active negative rotation about fixed axes. This feature explains the reverse order and negative sign of the Euler angles calculated with PALES compared to other programs based on the Y′ and mobile convention.

Finally, we have translated all numerical results given in Table 1 for the data collected on the extracellular domain of the PknB protein according to the new equivalencies listed in Table 3. Table 4 lists the Euler angles values calculated by all programs, and their values harmonized according to Table 3. The comparison of the harmonized Euler angle values shows that the orientations calculated either for the alignment tensor (MODULE, REDCAT, PALES, DCserver) or for the rotational diffusion tensor (TENSOR2, ROTDIF) are quasi identical, regardless of which program was used. Moreover, the harmonization enables the straightforward comparison of the relative orientation of the alignment and the rotational diffusion tensors. It appears that they are very similar, with the orientation of axial axes differing by only 13°. Not surprisingly, the discrepancy between the positions of the rhombic components is higher (35°).

Conclusion

We have established the equivalencies between the Euler angles calculated with commonly used software packages that derive or predict tensorial interactions in liquid NMR. In particular, we have established the numerical correspondence between Euler angles of the X′ and Y′ rotation schemes. The equivalencies listed in this report should facilitate the study of biomolecules, in particular in the case of high molecular weight proteins or protein complexes where oriental long-range restraints are widely used. Back in 1955, Robert Mulliken stated “It has been suggested by several people that it would be desirable, in the theoretical discussion of rigid rotor functions, to agree on a single standard way of choosing Eulerian angles. However, since any such standardization should have the agreement of other groups in addition to the spectroscopists, it is proposed that such a cooperative agreement be sought at a later date.” (Mulliken 1955). Sixty years later, we obviously still are in the waiting period before a decision is made and the present work should help with these notions in the field of biomolecular NMR. Conversion tables have been made accessible at the following address: http://www.cbs.cnrs.fr/SP/Demene/Conversion-Euler-Tensors.htm.

References

Almond A, Axelsen JB (2002) Physical interpretation of residual dipolar couplings in neutral aligned media. J Am Chem Soc 124(34):9986–9987

Azurmendi HF, Bush CA (2002) Tracking alignment from the moment of inertia tensor (TRAMITE) of biomolecules in neutral dilute liquid crystal solutions. J Am Chem Soc 124(11):2426–2427

Barthe P, Mukamolova GV, Roumestand C, Cohen-Gonsaud M (2010) The structure of PknB extracellular PASTA domain from mycobacterium tuberculosis suggests a ligand-dependent kinase activation. Structure 18(5):606–615

Berlin K, O'Leary DP, Fushman D (2010) Structural assembly of molecular complexes based on residual dipolar couplings. J Am Chem Soc 132(26):8961–8972

Bewley CA, Clore GM (2000) Determination of the relative orientation of the two halves of the domain-swapped dimer of cyanovirin-N in solution using dipolar couplings and rigid body minimization. J Am Chem Soc 122(25):6009–6016

Blake-Hall J, Walker O, Fushman D (2004) Characterization of the overall rotational diffusion of a protein from 15N relaxation measurements and hydrodynamic calculations. Methods Mol Biol 278:139–160

Cornilescu GB, Bax A (2000) Measurement of proton, nitrogen and carbonyl chemical shift shielding anisotropies in a protein dissolved in a dilute liquid crystalline phase. J Am Chem Soc 122(41):10143–10154

Déméné H, Tsan P, Gans P, Marion D (2000) NMR determination of the magnetic susceptibility anisotropy of cytochrome c' of *Rhodobacter capsulatus* by 1 J (HN) dipolar coupling constants measurement: characterization of its monomeric state in solution. J Phys Chem B 104(11):2559–2569

Déméné H, Ducat T, Barthe P, Delsuc MA, Roumestand C (2002) Structure refinement of flexible proteins using dipolar couplings: application to the protein p8MTCP1. J Biomol NMR 22(1):47–56

Déméné H, Ducat T, De Guillen K, Birck C, Aymerich S, Kochoyan M, Declerck N (2008) Structural mechanism of signal transduction between the RNA-binding domain and the phosphotransferase system regulation domain of the LicT antiterminator. J Biol Chem 283(45):30838–30849

Dosset P, Hus JC, Blackledge M, Marion D (2000) Efficient analysis of macromolecular rotational diffusion from heteronuclear relaxation data. J Biomol NMR 16(1):23–28

Dosset P, Hus JC, Marion D, Blackledge M (2001) A novel interactive tool for rigid-body modeling of multi-domain macromolecules using residual dipolar couplings. J Biomol NMR 20(3):223–231

Fernandes MX, Bernado P, Pons M, Garcia de la Torre J (2001) An analytical solution to the problem of the orientation of rigid particles by planar obstacles. Application to membrane systems and to the calculation of dipolar couplings in protein NMR spectroscopy. J Am Chem Soc 123(48):12037–12047

Ferrarini A (2003) Modeling of macromolecular alignment in nematic virus suspensions. Application to the prediction of NMR residual dipolar couplings. J Chem Phys B 107(31):7923–7931

Fushman D, Xu R, Cowburn D (1999) Direct determination of changes of interdomain orientation on ligation: use of the orientational dependence of 15N NMR relaxation in Abl SH(32). Biochemistry 38(32):10225–10230

Ghose R, Fushman D, Cowburn D (2001) Determination of the rotational diffusion tensor of macromolecules in solution from nmr relaxation data with a combination of exact and approximate methods–application to the determination of interdomain orientation in multidomain proteins. J Magn Reson 149(2):204–217

Hansen MR, Mueller L, Pardi A (1998) Tunable alignment of macromolecules by filamentous phage yields dipolar coupling interactions. Nat Struct Biol 5(12):1065–1074

Hus JC, Salmon L, Bouvignies G, Lotze J, Blackledge M, Bruschweiler R (2008) 16-fold degeneracy of peptide plane orientations from residual dipolar couplings: analytical treatment and implications for protein structure determination. J Am Chem Soc 130(47):15927–15937

Hwang PM, Skrynnikov NR, Kay LE (2001) Domain orientation in beta-cyclodextrin-loaded maltose binding protein: diffusion anisotropy measurements confirm the results of a dipolar coupling study. J Biomol NMR 20(1):83–88

Manival X, Yang Y, Strub MP, Kochoyan M, Steinmetz M, Aymerich S (1997) From genetic to structural characterization of a new class of RNA-binding domain within the SacY/BglG family of antiterminator proteins. EMBO J 16(16):5019–5029

Mueller L (2011) Tensors and rotations in NMR. Concepts Magn Reson 38A(5):221–235

Mueller GA, Choy WY, Yang D, Forman-Kay JD, Venters RA, Kay LE (2000) Global folds of proteins with low densities of NOEs using residual dipolar couplings: application to the 370-residue maltodextrin-binding protein. J Mol Biol 300(1):197–212

Mulliken R (1955) Report on notation for the spectra of polyatomic molecules. J Chem Phys 23(11): 1997–2011

Rose M (1955) Elementary theory of angular momentum. Wiley, New York

Ruckert M, Otting G (2000) Alignment of biological macromolecules in novel nonionic liquid crystallinne media for NMR measurement. J Am Chem Soc 122(32):7793–7797

Ryabov Y, Fushman D (2007) Structural assembly of multidomain proteins and protein complexes guided by the overall rotational diffusion tensor. J Am Chem Soc 129(25):7894–7902

Ryabov Y, Suh JY, Grishaev A, Clore GM, Schwieters CD (2009) Using the experimentally determined components of the overall rotational diffusion tensor to restrain molecular shape and size in NMR structure determination of globular proteins and protein–protein complexes. J Am Chem Soc 131(27):9522–9531

Schmidt-Rohr K, Spiess HW (1994) Multidimensional solid-state NMR and polymers. Academic Press Limited, London, pp 443–447

Schwieters CD, Kuszewski JJ, Tjandra N, Clore GM (2003) The Xplor-NIH NMR molecular structure determination package. J Magn Reson 160(1):65–73

Skrynnikov NR, Goto NK, Yang D, Choy WY, Tolman JR, Mueller GA, Kay LE (2000) Orienting domains in proteins using dipolar couplings measured by liquid-state NMR: differences in solution and crystal forms of maltodextrin binding protein loaded with beta-cyclodextrin. J Mol Biol 295(5):1265–1273

Tjandra N, Bax A (1997) Direct measurement of distances and angles in biomolecules by NMR in a dilute liquid crystalline medium. Science 278(5340):1111–1114

Tjandra N, Garrett DS, Gronenborn AM, Bax A, Clore GM (1997a) Defining long range order in NMR structure determination from the dependence of heteronuclear relaxation times on rotational diffusion anisotropy. Nat Struct Biol 4(6):443–449

Tjandra N, Omichinski JG, Gronenborn AM, Clore GM, Bax A (1997b) Use of dipolar 1H-15N and 1H-13C couplings in the structure determination of magnetically oriented macromolecules in solution. Nat Struct Biol 4(9):732–738

Valafar H, Prestegard JH (2004) REDCAT: a residual dipolar coupling analysis tool. J Magn Reson 167(2):228–241

van Tilbeurgh H, Manival X, Aymerich S, Lhoste JM, Dumas C, Kochoyan M (1997) Crystal structure of a new RNA-binding domain from the antiterminator protein SacY of *Bacillus subtilis*. EMBO J 16(16):5030–5036

Vincent B, Morellet N, Fatemi F, Aigrain L, Truan G, Guittet E, Lescop E (2012) The closed and compact domain organization of the 70-kDa human cytochrome P450 reductase in its oxidized state as revealed by NMR. J Mol Biol 420(4–5):296–309

Walker O, Varadan R, Fushman D (2004) Efficient and accurate determination of the overall rotational diffusion tensor of a molecule from (15)N relaxation data using computer program ROTDIF. J Magn Reson 168(2):336–345

Wolf AA (1969) Rotation operators. Am J Chem Phys 37(5):531–536

Wu B, Petersen M, Girard F, Tessari M, Wijmenga SS (2006) Prediction of molecular alignment of nucleic acids in aligned media. J Biomol NMR 35(2):103–115

Yang Y, Declerck N, Manival X, Aymerich S, Kochoyan M (2002) Solution structure of the LicT-RNA antitermination complex: CAT clamping RAT. EMBO J 21(8):1987–1997

Zweckstetter M, Bax A (2000) Prediction of sterically induced alignment in a dilute liquid crystalline phase: aid to protein structure determination by NMR. J Am Chem Soc 122(2000): 3791–3792

Zweckstetter M, Hummer G, Bax A (2004) Prediction of charge-induced molecular alignment of biomolecules dissolved in dilute liquid-crystalline phases. Biophys J 86(6):3444–3460

Zweckstetter M, Schnell JR, Chou JJ (2005) Determination of the packing mode of the coiled-coil domain of cGMP-dependent protein kinase Ialpha in solution using charge-predicted dipolar couplings. J Am Chem Soc 127(34):11918–11919